

# Clusterin and Related Scoring Index as Potential Early Predictors of Response to Sorafenib in Hepatocellular Carcinoma

Satoshi Narahara <sup>1</sup>, Takehisa Watanabe <sup>1</sup>, Katsuya Nagaoka <sup>1</sup>, Nahoko Fujimoto,<sup>1</sup> Yoki Furuta,<sup>1</sup> Kentaro Tanaka,<sup>1</sup> Takayuki Tokunaga,<sup>1</sup> Takeshi Kawasaki,<sup>1</sup> Yoko Yoshimaru,<sup>1</sup> Hiroko Setoyama,<sup>1</sup> Kentaro Oniki,<sup>2</sup> Junji Saruwatari,<sup>2</sup> Masakuni Tateyama,<sup>1</sup> Hideaki Naoe,<sup>1</sup> Motohiko Tanaka,<sup>1,3</sup> Yasuhito Tanaka <sup>1</sup>, and Yutaka Sasaki <sup>1,4</sup>

Advanced hepatocellular carcinoma (HCC) remains a highly lethal malignancy, although several systemic therapeutic options are available, including sorafenib (SFN), which has been one of the standard treatment agents for almost a decade. As early prediction of response to SFN remains challenging, biomarkers that enable early prediction using a clinically feasible method are needed. Here, we report that the serum secretory form of clusterin (sCLU) protein and its related predictive index are potential beneficial biomarkers for early prediction of SFN response. Using high-throughput screening and subsequent multivariate analysis in the derivation cohort, we found that changes in the concentrations of CLU, vascular cell adhesion molecule-1 (VCAM1), and  $\alpha$ -fetoprotein were significantly associated with response to SFN. Furthermore, we confirmed that an increase in CLU serum level 1 month after treatment initiation was significantly associated with shorter progression-free survival. In addition, “NR-index,” which comprises these proteins, was evaluated as a tool for accurately predicting the efficacy of SFN and confirmed in the validation cohort. We also established SFN-resistant HepG2 cells (HepG2-SR) and found that sCLU significantly increased in HepG2-SR cells compared with normal HepG2 cells, and confirmed that HepG2-SR cells treated with SFN were resistant to apoptosis. The mechanism underlying activation of sCLU expression in acquired SFN resistance involves aberrant signaling and expression of Akt, mammalian target of rapamycin (mTOR), and a nutrient-related transcription factor, sterol regulatory element binding protein 1c (SREBP-1c). Furthermore, the PI3K and mTOR inhibitor BEZ235 markedly decreased sCLU expression in HepG2-SR cells. **Conclusion:** These results suggest that measurement of sCLU serum levels and the sCLU-related NR-index are promising clinical tools for the early prediction of SFN response in HCC. Additionally, sCLU-overexpressing HCC might be susceptible to mTOR inhibition. (*Hepatology Communications* 2022;6:1198-1212).

**H**epatocellular carcinoma (HCC) is the sixth most common and third most lethal malignancy in the world, and the disease is common in Asia and Africa.<sup>(1)</sup> Current treatments for HCC include surgical resection, liver transplantation, radiofrequency ablation, transcatheter arterial

chemoembolization, and molecular-targeted agents (MTAs).<sup>(2)</sup>

Sorafenib (SFN), a multikinase inhibitor of growth factor signaling pathways, inhibits the vascular endothelial growth factor and mitogen-activated protein kinase (MAPK) pathways, particularly Raf activation,

*Abbreviations:* AFP,  $\alpha$ -fetoprotein; AUC, area under the curve; CI, confidence interval; CRELD2, cysteine-rich with endothelial growth factor-like domain protein; ELISA, enzyme-linked immunosorbent assay; GSEA, gene-set enrichment analysis; HCC, hepatocellular carcinoma; HepG2-SR, sorafenib-resistant HepG2 cells; HR, hazard ratio; MAPK, mitogen-activated protein kinase; mRNA, messenger RNA; MTA, molecular-targeted agent; mTOR, mammalian target of rapamycin; OR, odds ratio; OS, overall survival; p-mTOR, phosphorylated mammalian target of rapamycin; PFS, progression-free survival; PI3K, phosphoinositide 3-kinase; ROC, receiver operating characteristic; sCLU, secretory form of clusterin; siRNA, small interfering RNA; SFN, sorafenib; SREBP1c, sterol regulatory element binding protein 1c; VCAM1, vascular cell adhesion molecule-1.

Received July 15, 2021; accepted November 10, 2021.

Additional Supporting Information may be found at [onlinelibrary.wiley.com/doi/10.1002/hep4.1872/supinfo](https://onlinelibrary.wiley.com/doi/10.1002/hep4.1872/supinfo).

Supported by the Japan Society for the Promotion of Science (Grants-in-Aid for Scientific Research: 18K07945, 18K15820, 19K17403, 21K07904, and 18H02798).

© 2021 The Authors. *Hepatology Communications* published by Wiley Periodicals LLC on behalf of American Association for the Study of Liver Diseases. This is an open access article under the terms of the Creative Commons Attribution-NonCommercial-NoDerivs License, which permits use and distribution in any medium, provided the original work is properly cited, the use is non-commercial and no modifications or adaptations are made.

which controls cell proliferation.<sup>(3-5)</sup> After two randomized controlled studies demonstrated the effectiveness of SFN at prolonging both overall survival (OS) and time to progression,<sup>(4,5)</sup> SFN was approved as a first-line treatment and has become the primary MTA for treatment of advanced HCCs over the past decade. Regorafenib, cabozantinib, and ramucirumab were then approved as treatments subsequent to SFN and lenvatinib. Recently, atezolizumab (atezo) plus bevacizumab (bev) has become available as a first-line treatment for most patients with advanced HCC, Child-Pugh class A, ECOG PS0-1.<sup>(6)</sup> However, where there is contraindication to atezo and/or bev, MTAs including SFN or lenvatinib may be offered as first-line treatment, according to American Society of Clinical Oncology (ASCO) guideline 2020.<sup>(7)</sup> In addition, following first-line treatment with atezo+bev, second-line treatment with MTAs (i.e., SFN, lenvatinib, cabozantinib, or regorafenib) are recommended.<sup>(7)</sup> Furthermore, several meta-analyses of randomized controlled trials have shown SFN to be more beneficial in hepatitis C virus-positive HCCs.<sup>(8-10)</sup> Taken all together, SFN is still in constant demand as the first-line and second-line agent for HCC systemic treatment.<sup>(7,11)</sup> Thus, improving the outcomes for patients with advanced HCCs will require the development of strategies that enable the early prediction of treatment response to SFN and inform the switch to other therapies as quickly as possible before failure of SFN treatment. Several studies have identified predictive markers of SFN efficacy by analyzing the associations between potential markers and patient

outcomes.<sup>(12,13)</sup> However, because of the complexity of patient backgrounds and the heterogeneity of HCC, it has been difficult to establish biomarkers that enable prediction of the response to SFN before the start of treatment.

In this study, we aimed to identify serum biomarkers and establish a formula for predicting SFN treatment response at an early stage after treatment initiation using paired serum samples from patients with advanced HCC. In addition, we clarified the molecular mechanism underlying SFN resistance using sorafenib-resistant HepG2 (HepG2-SR) cells.

## Materials and Methods

### STUDY DESIGN

A total of 126 patients who received SFN therapy at Kumamoto University Hospital from June 2008 to April 2019 participated in this study. Tumor response at 3 months after treatment initiation was evaluated based on modified response evaluation criteria in solid tumors (mRECIST). Patients were divided into two groups: a nonresponder (NR) group (n = 42), defined as patients with progressive disease; and a responder (R) group (n = 84), defined as patients exhibiting complete response, partial response, or stable disease.

Among the entire study group, 68 paired serum samples (NR = 35, R = 33) from before and 1 month after initiation of SFN treatment were available for this study. Serum was collected at almost the same time in

*View this article online at [wileyonlinelibrary.com](http://wileyonlinelibrary.com).*

*DOI 10.1002/hep4.1872*

*Potential conflict of interest: Nothing to report.*

### ARTICLE INFORMATION:

From the <sup>1</sup>Department of Gastroenterology and Hepatology, Faculty of Life Sciences, Kumamoto University, Kumamoto, Japan; <sup>2</sup>Department of Pharmacology and Therapeutics Graduate School of Pharmaceutical Sciences, Kumamoto University, Kumamoto, Japan; <sup>3</sup>Public Health and Welfare Bureau, City of Kumamoto, Kumamoto, Japan; <sup>4</sup>Department of Health and Nutrition, Faculty of Health Management, Nagasaki International University, Nagasaki, Japan.

### ADDRESS CORRESPONDENCE AND REPRINT REQUESTS TO:

Yutaka Sasaki, M.D., Ph.D.  
Department of Health and Nutrition  
Faculty of Health Management  
Nagasaki International University

2825-7 Huis Ten Bosch Machi  
Sasebo City, Nagasaki 859-3298, Japan  
E-mail: [sasakiy@kumamoto-u.ac.jp](mailto:sasakiy@kumamoto-u.ac.jp)  
Tel.: +81-956-20-5569

the early morning before meals to avoid the influence of diurnal variation. Eighteen patients were randomly selected from the NR group and R group, and these 36 patients constituted the derivation cohort, whereas 11 patients were randomly selected from each group and 22 patients constituted the validation cohort (Supporting Fig. S1, Supporting Table S1).

Written informed consent was obtained from all participants. The study protocol was approved by the Institutional Review Board of Kumamoto University (Approval no. 1094).

## PROTEOME ANALYSIS

Proteomic analyses of serum proteins were carried out using Proteome Profiler antibody arrays (R&D Systems, Minneapolis, MN), namely the Human Angiogenesis Array kit (ARY007), Human Soluble Receptor Array kit (ARY012), and Human Adipokine Array kit (ARY024). Each examination was performed according to the respective protocol. Briefly, serum samples for use with each kit were applied to nitrocellulose membranes with bound capture antibodies for target proteins and incubated for 24 hours in a refrigerated room followed by removing serum from the membrane and assaying immediately. Samples were analyzed using a LAS system (Ez-Capture MG; ATTO Corp., Tokyo, Japan). Measured signals are presented as percentage of the negative control (0%) and positive control (100%). We selected proteins in an unbiased manner that met the following criteria: (1) significant difference ( $P < 0.05$ ) in rate of change in value between the R group and NR group; (2) exhibit >1.5-fold difference between before and 1 month after SFN treatment initiation; and (3) measured value >5%.

## ENZYME-LINKED IMMUNOSORBENT ASSAY (ELISA) ANALYSIS

Levels of the serum secretory form of clusterin (sCLU), vascular cell adhesion molecule-1 (VCAM1), thrombospondin-1, E-selectin, angiogenin, matrix metalloproteinase-9, adiponectin, tissue inhibitor of metalloproteinases-1, insulin-like growth factor-binding protein-2, insulin-like growth factor-binding protein-3, and complement factor D were determined using a Quantikine enzyme-linked immunosorbent

assay (ELISA) kit (R&D Systems, Minneapolis, MN). Levels of dipeptidyl peptidase-4 and fetuin B were determined using a DuoSet ELISA kit (R&D Systems, Minneapolis, MN). Levels of cysteine-rich with endothelial growth factor-like domain protein (CRELD2), cadherin-13, and scavenger receptor expressed by endothelial cells-1 were determined using a RayBio ELISA kit (RayBiotech, Peachtree Corners, GA), and levels of cathepsin S and cathepsin D were determined using a PicoKine ELISA kit (Boster Biological Technology, Pleasanton, CA). The protocols of the respective kits were followed. Briefly, 100  $\mu$ L of diluted serum was added to the indicated wells and incubated at room temperature for 2 hours. After washing four times, substrate solution was added and the mixture was incubated for 20 minutes at room temperature, followed by addition of stop solution. Finally, the absorbance at 450 nm of duplicate samples was monitored using a microplate reader (iMark Microplate Absorbance Reader; BioRad, Hercules, CA).

## MICROARRAY ANALYSIS

Genome-wide expression analysis was performed using a GeneChip Human Genome Array U133 Plus 2.0 in combination with a GeneChip hybridization, wash, and stain kit (Affymetrix, Santa Clara, CA). We prepared two cell lines: HepG2 cells and HepG2-SR cells. Total RNA was extracted from cells using TRIzol reagent and cleaned using a RNeasy Plus Mini kit (Qiagen, Germantown, MD). Biotin-labeled complementary DNA (cDNA) was synthesized by *in vitro* transcription reaction from the total RNA according to the protocol. Gene-expression microarray analysis was performed using GeneChip Human Genome U133 Plus 2.0 Array with a GeneChip hybridization, wash, and stain kit (Thermo Fisher Scientific, Waltham, MA) at Takara Bio Inc., Japan.<sup>(14)</sup> Data were annotated using GeneSpring GX software (Agilent, Santa Clara, CA). Gene-set enrichment analysis (GSEA) was performed using GSEA software, version 4.0, obtained from the Broad Institute of MIT and Harvard University (<http://www.broadinstitute.org/gsea/>).

## CELL CULTURE

HepG2, Huh7, and Hep3B cells were cultured in Dulbecco's modified Eagle's medium (DMEM) supplemented with 10% (vol/vol) heat-inactivated fetal

bovine serum (FBS). HepG2-SR were established by culturing HepG2 cells with long-term exposure to SFN at gradually increasing concentrations. For the experiments involving SFN treatment using HepG2-SR cells, we challenged HepG2-SR cells with SFN up until 24 hours before the medium change. We then cultured the HepG2-SR cells in regular medium (high glucose DMEM plus 10% heat-inactivated FBS) without SFN for 24 hours, and afterward, retreated the cells with SFN. For small interfering RNA (siRNA)-mediated knockdown, Invitrogen Silencer Select siCLU (s3157) was used for *CLU* knockdown. Invitrogen Silencer Select (SREBF1 s129) was used for sterol regulatory element binding protein 1 (*SREBP1*) knockdown. Invitrogen Silencer Select Negative Control #1 siRNA (Thermo Fisher Scientific, Waltham, MA) was used as the siControl. Cells were transfected with siRNAs for 48 hours using Lipofectamine RNAiMAX reagent (Thermo Fisher Scientific).

## CELL PROLIFERATION ASSAY

Cell proliferation was measured using a Cell Counting Kit-8 (Dojindo, Kumamoto, Japan) containing tetrazolium salt, WST-8 (2-[2-methoxy-4-nitrophenyl]-3-[4-nitrophenyl]-5-[2,4-disulfophenyl]-2-H-tetrazolium, monosodium salt). Cells were seeded in a 96-well plate at a density of 3,000-5,000 cells/well. To determine the number of live cells, WST-8 solution was added during the final 1 hour of incubation, and the absorbance of each well was measured using a microplate reader at a wavelength of 450 nm.  $EC_{50}$  values were calculated using GraphPad Prism 8 software.

## REAL-TIME POLYMERASE CHAIN REACTION ANALYSIS

Quantitative polymerase chain reaction (PCR) analysis was performed as previously reported.<sup>(15)</sup> Total RNA was extracted from cells using TRIzol reagent (Thermo Fisher Scientific, Waltham, MA). cDNAs were produced using a PrimeScript RT reagent kit with gDNA Eraser (Takara Bio, Shiga, Japan). Quantitative reverse-transcription PCR was performed using TB Green Premix Ex Taq (Takara Bio) and Thermal Cycler Dice Real Time System Lite (Takara Bio). Data are expressed as the mean  $\pm$  SD. Statistical analyses were performed using two-tailed Student *t* tests. The primers used in this study are listed in Supporting Table S2.

## WESTERN BLOT ANALYSIS

For detection of sCLU, cytoplasmic components were isolated using a LysoPure Nuclear and Cytoplasmic Extractor kit (Fujifilm Wako Pure Chemical Corporation, Osaka, Japan), and nuclear components were discarded. Cytoplasmic lysates were separated by sodium dodecyl sulfate-polyacrylamide gel electrophoresis (SDS-PAGE), and the proteins were transferred onto polyvinylidene fluoride membranes. Blots were incubated with respective primary antibodies overnight at 4°C, followed by incubation with corresponding secondary antibodies for 1 hour. Proteins were visualized by enhanced chemiluminescence using EzWestLumi Plus and Ez-Capture MG (ATTO Corp., Tokyo, Japan). Anti-CLU (sc-5289) and anti-GAPDH (sc-32233) antibodies were purchased from Santa Cruz Biotechnology (Dallas, TX). Anti-p-Akt (4060), anti-pan Akt (2920), anti-p-Erk (1/2) (9106), and anti-phosphorylated mammalian target of rapamycin (p-mTOR) (5536) antibodies were purchased from Cell Signaling Technology (Danvers, MA). Anti-Erk (1/2) antibody (MAB1576) was purchased from R&D Systems (Minneapolis, MN). Cleaved Caspase-3 antibody (#9661) was purchased from Cell Signaling Technology (Danvers, MA).

## IMMUNOFLUORESCENT STAINING

Cells were fixed with 100% methanol for 5 minutes at room temperature. After blocking with 3% bovine serum albumin, the cells were incubated with anti-SREBF1 (14088-1AP) (Proteintech, IL) or anti-CLU (sc-5289) (Santa Cruz Biotechnology, Dallas, TX) overnight at 4°C. The cells were washed with phosphate-buffered saline, and incubated with Alexa Fluor 594-labeled anti-rabbit (1:1,000) secondary antibodies (Invitrogen; Thermo Fisher Scientific) for 60 minutes at room temperature. Samples were analyzed by fluorescence microscope system (KEYENCE, Osaka, Japan), and the fluorescence intensity was analyzed using the BZ-X Analyzer.

## STATISTICAL ANALYSES

Results are expressed as the mean  $\pm$  SD or median (minimum-maximum). The statistical significance of differences was assessed using two-tailed Student *t* test. Relationships between the R and NR groups and serum proteins were assessed using the  $X^2$  test. Logistic

regression analyses were designed to identify the most relevant predictors for NR. OS and progression-free survival (PFS) times were calculated according to the Kaplan–Meier method, with differences between the two groups analyzed using log-rank tests. To confirm the precision of the NR-index, bootstrap analyses were performed using 1,000 replicated data sets randomly sampled from the 50 patients in the derivation and validation cohorts. The generated data sets were stratified according to the study population to ensure a representative study population distribution using the individual as the sampling unit.<sup>(16)</sup> All statistical analyses using the clinical data were performed using IBM SPSS Statistics 24 software (IBM, Armonk, NY), with  $P < 0.05$  considered statistically significant unless otherwise stated.

## DATABASE ANALYSES

Expression profiles of CLU in the liver were determined using immunohistochemistry data for cancer and human liver tissue from the *Human Protein Atlas* ([www.proteinatlas.org/ENSG00000120885-CLU/pathology/tissue/liver+cancer#img](http://www.proteinatlas.org/ENSG00000120885-CLU/pathology/tissue/liver+cancer#img)).

## Results

### PROTEOME ANALYSIS IDENTIFIED THREE CANDIDATE PROTEINS TO PREDICT THE TREATMENT RESPONSE TO SFN

We aimed to identify a serum biomarker for early prediction of the response to SFN treatment. To reduce interference associated with the complexity of patient backgrounds and ensure the clear determination of the effect of SFN, we focused on the rate of change in the concentration of each serum protein.

First, to comprehensively analyze changes in serum protein concentrations, a proteome array was used, using five paired serum samples (pretreatment and 1 month after treatment initiation) each from the R or NR group in the derivation cohort. We quantified 232 serum proteins in the array to calculate the rate of change for each protein and then compared the rates between the two groups (Fig. 1A). To narrow down the list of candidate proteins, technical duplicates of the proteome analysis were conducted, and candidates were selected based on the criteria described in the “Proteome Analysis”

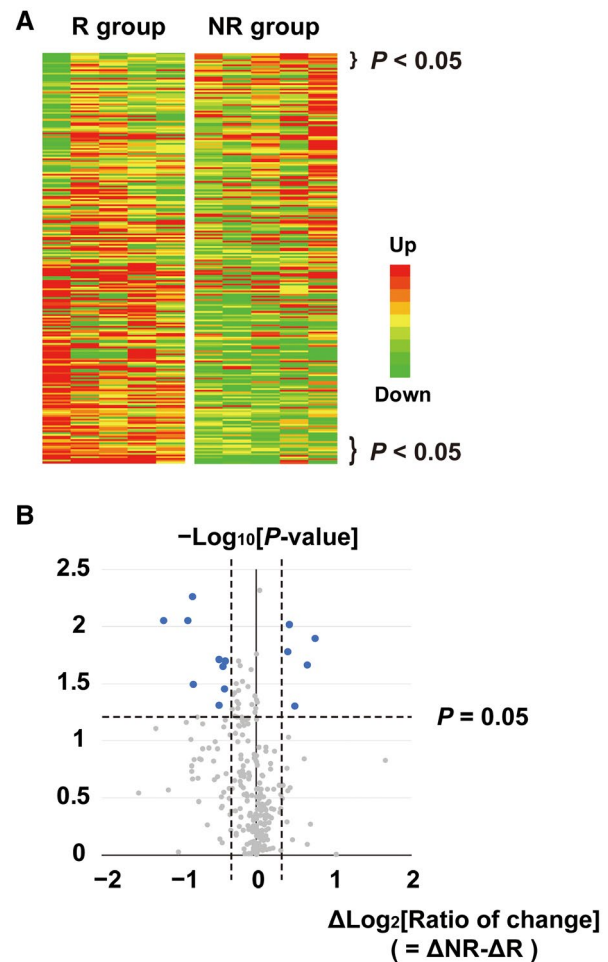


**FIG. 1.** Proteome analysis to identify proteins exhibiting significant changes in serum concentration in response to SFN treatment. (A) Results of  $t$ -tests analyzing rates of change in protein concentration before and after treatment initiation. Candidate proteins were sorted according to the significance of the difference between the 2 groups. (B) Candidate proteins were selected based on the results of technical duplicate proteome analyses using the following criteria: (1) exhibit significant difference ( $P < 0.05$ ) in rate of change between the R group and NR group; (2) exhibit a >1.5-fold difference between before and 1 month after initiation of SFN treatment; and (3) exhibit a measured value >5%. A total of 14 proteins (blue dots) were selected from 2 proteome analyses, and 4 proteins were detected in 1 of the analyses.

section. A total of 14 candidate proteins (blue dots in Fig. 1B) were identified in two proteome analyses, and four proteins were identified in one of the analyses.

Using ELISA, we then compared the rates of change among the 18 total proteins between the R group ( $n = 18$ ) and NR group ( $n = 18$ ) in the derivation cohort (Fig. 2, Supporting Fig. S2). The rates

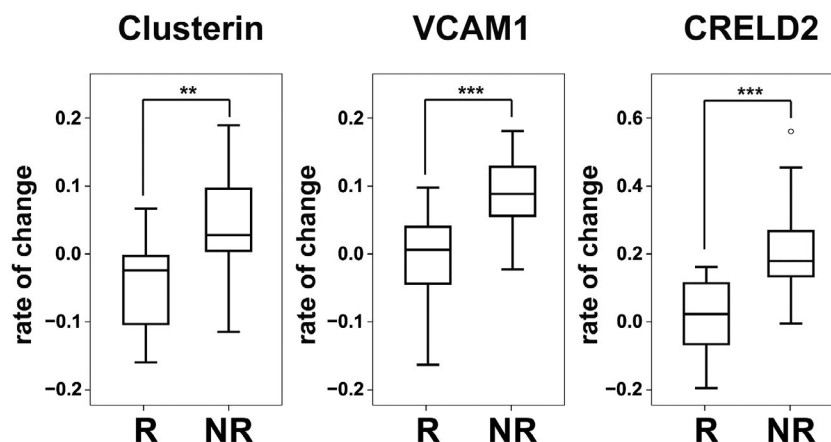


**FIG. 2.** Changes in serum CLU, VCAM1, and CRELD2 concentrations in response to SFN treatment differed significantly between the R group and NR group. Box-and-whisker plots of 3 proteins exhibiting a significant change. The rates of change in CLU, VCAM1, and CRELD2 concentration were significantly higher in the NR group than the R group 1 month after treatment initiation (R = 18, NR = 18). \*\* $P < 0.01$ , \*\*\* $P < 0.001$ . Abbreviations: CLU, clusterin; VCAM1, vascular cell adhesion molecule-1; CRELD2, cysteine-rich with EGF-like domain protein 2.

of change differed significantly between the two groups for three proteins: CLU ( $P = 0.002$ ), VCAM1 ( $P < 0.001$ ), and CRELD2 ( $P < 0.001$ ) (Fig. 2).

## NR-INDEX PREDICTED THE PROGNOSIS OF SFN-TREATED PATIENTS WITH HCC

We also found that the rate of change in the serum  $\alpha$ -fetoprotein (AFP) level significantly differed between the two groups, whereas the background and tumor characteristics of the patients at baseline did not show significant differences (Table 1, Supporting Table S1). Univariate and multivariate analyses with the three candidate proteins and AFP indicated that three of the factors contributed significantly to no response: CLU (odds ratio [OR] = 12.2,  $P = 0.035$ ), VCAM1 (OR = 6.62,  $P = 0.045$ ), and AFP (OR = 12.2,  $P = 0.035$ ) (Table 2).

To establish a formula for predicting the therapeutic effect of SFN, we performed receiver operating characteristic (ROC) curve analysis for CLU, VCAM1, and AFP. The area under the curve (AUC) values for CLU, VCAM1, and AFP were 0.787, 0.840, and 0.812, respectively (Supporting Fig. S3A, Supporting Table S3A). We then determined that the cutoff values according to the least-squares method were 0.0020, 0.0398, and 0.0992, respectively. The ORs for CLU, VCAM1, and AFP were 9.09 ( $P = 0.003$ ), 20.8 ( $P < 0.001$ ), and 13.0 ( $P = 0.001$ ), respectively

**TABLE 1. RATES OF CHANGE IN SERUM MARKERS IN RESPONSE TO SFN TREATMENT**

	R Group (n = 18)	NR Group (n = 18)	<i>P</i> Value
Albumin	0.002 ± 0.062	0 ± 0.149	0.890
Bilirubin	0.097 ± 0.308	0.178 ± 0.383	0.187
Aspartate transaminase	0.143 ± 0.288	0.173 ± 0.522	0.681
Alanine transaminase	0.094 ± 0.399	0.131 ± 0.629	0.689
Lactate dehydrogenase	0.154 ± 0.176	0.168 ± 0.317	0.753
Alkaline phosphatase	0.073 ± 0.154	0.090 ± 0.265	0.651
Gamma-glutamyl transpeptidase	-0.02 ± 0.318	0.087 ± 0.326	0.055
Platelet	-0.09 ± 0.330	-0.06 ± 0.287	0.522
Prothrombin time	-0.02 ± 0.164	0.009 ± 0.124	0.186
AFP	-0.09 ± 0.656	0.200 ± 0.513	0.007
PIVKA-II	0.508 ± 1.102	0.754 ± 0.959	0.174

Note: Values are expressed as the logarithm rate of change in each parameter before and 1 month after SFN treatment initiation.

(Table 3). Moreover, to improve the accuracy of prediction for SFN efficacy, we created a prognostic index based on the results of the linear regression analysis using the determined cutoff values. Because the difference in regression coefficients was less than double,

**TABLE 2. UNIVARIATE AND MULTIVARIATE ANALYSIS ON FACTORS CONTRIBUTING TO SFN TREATMENT RESPONSE**

Rate of Change	Univariate Analysis			Multivariate Analysis		
	OR	95% CI	PValue	OR	95% CI	PValue
CLU	6.76	1.57-29.4	0.008	12.2	1.19-125	0.035
VCAM1	12.2	2.54-58.8	0.001	6.62	1.04-41.7	0.045
CRELD2	6.76	1.57-29.4	0.008			N.S.
AFP	6.76	1.57-29.4	0.008	12.2	1.19-125	0.035

**TABLE 3. RESULTS OF X-SQUARE TEST AND LINEAR REGRESSION ANALYSIS**

Rate of Change	$\chi^2$ Test				Linear Regression Analysis	
	Cutoff Value	OR	95% CI	PValue	Regression Coefficient	PValue
CLU	0.002	9.09	2.00-41.7	0.003	0.262	0.048
VCAM1	0.0398	20.8	3.44-125	<0.001	0.383	0.007
AFP	0.0992	13.0	2.59-66.7	0.001	0.405	0.002

when the rate of change in CLU, VCAM1, or AFP concentration exceeds the respective cutoff value, it is counted as 1 point in order to simplify a formula, with the sum of these points defined as the NR-index. The AUC of the NR-index was 0.926, which was larger than the AUC of each protein alone (Supporting Fig. S3A, Supporting Table S3A). The 36 patients examined by ELISA (R = 18, NR = 18) as the derivation cohort were then categorized into two groups based on the NR-index, specifically, 0 or 1 point as the low-NR index group (n = 19), and 2 or 3 points as the high-NR index group (n = 17) (Fig. 3A). The NR and R groups could be distinguished with statistical significance based on the NR index. The median OS and PFS times were significantly longer for patients in the low-NR index group compared with the high-NR index group (OS: low-NR index group = 24.7 months, high-NR index group = 6.5 months [hazard ratio (HR) = 1.694,  $P = 0.004$ ]; and PFS: low-NR index group = 6.2 months, high-NR index group = 1.3 months [HR = 1.990,  $P < 0.001$ ]) (Fig. 3B,C).

Finally, we randomly selected another 22 cases (R = 11, NR = 11) for a validation cohort study to confirm that the response to SFN 3 months after treatment initiation can be accurately predicted using the NR-index. When ROC curves were generated based on the cutoff values of each protein, the cutoff values for CLU and AFP had significant diagnostic potential (CLU:  $P < 0.001$ , AFP:  $P = 0.020$ ), and the

cutoff value for VCAM1 showed a trend toward useful diagnostic potential ( $P = 0.079$ ). In addition, the combination of two or even three proteins had a larger AUC and a more significant diagnostic value than each protein alone (Supporting Fig. S3B, Supporting Table S3B). When we applied the NR-index to the validation cohort, the high-NR index group was significantly related to no response (Fig. 3D) and associated with a shorter PFS time, as shown in the derivation cohort. Whereas the median OS was 15.7 months in the low-NR index group and 6.9 months in the high-NR index group, the median PFS was 4.7 months in the low-NR index group and 1.4 months in the high-NR index group, with an HR of 3.784 ( $P = 0.006$ ) (Fig. 3E,F). Significant bias in AUC values among CLU, VCAM1, and AFP was not observed when we performed X-square analysis between every two proteins, using each cutoff value for the derivation cohort (Supporting Table S3C).

Furthermore, to confirm the results, a stratified non-parametric bootstrap analysis was performed. One thousand replicated data sets were randomly sampled from the 50 patients out of the derivation (n = 36) and validation (n = 22) cohort and stratified according to the study population to ensure a representative study population distribution using the individual as the sampling unit. The results confirmed that the NR-index contributed significantly to no response (OR = 41.67,  $P < 0.001$ , 95% confidence interval [CI] = 12.57-9.30  $\times 10^9$ ).

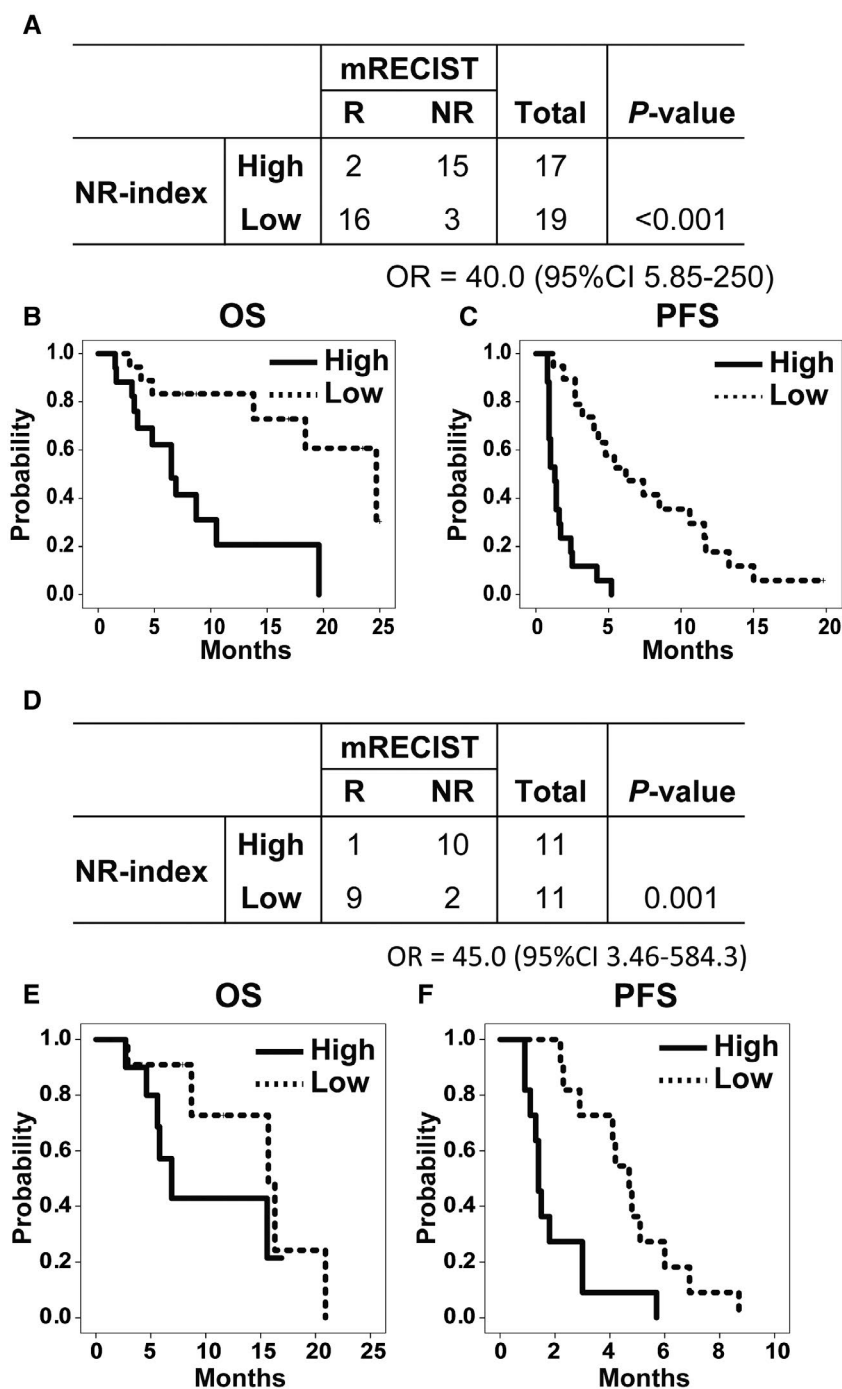


**FIG. 3.** NR index predicted prognosis of HCC patients treated with SFN. (A) Classification of 36 patients (R = 18, NR = 18) in the derivation cohort into 2 groups (low group: n = 19, high group: n = 17) based on NR-index indicated that the NR-index is a significant predictor of the SFN response ( $P < 0.001$ , OR = 40.0, 95% CI 5.85-250). (B, C) Kaplan-Meier curves for OS and PFS according to the NR-index. The NR-index was useful for discriminating SFN-treated patients who had a poor response to treatment. Both OS and PFS were significantly different (OS:  $P = 0.004$ , HR = 1.694; PFS:  $P < 0.001$ , HR = 1.990). (D) Classification of 22 patients (R = 11, NR = 11) in the validation cohort into 2 groups (low group: n = 11, high group: n = 11) based on NR-index indicated that the NR-index was a significant predictor as in the derivation cohort ( $P = 0.001$ , OR = 45.0, 95% CI 3.46-584.3). (E, F) Kaplan-Meier analysis of OS and PFS in the validation cohort. The PFS of the high-NR-index group was significantly shorter than that of the low-NR-index group ( $P = 0.006$ , HR = 3.784). Abbreviations: OR, odds ratio; SFN, sorafenib; OS, overall survival; PFS, progression-free survival; HR, hazard ratio.

## RELATIONSHIP BETWEEN CHANGE IN CLU CONCENTRATION AND PROGNOSIS

Thirty-six patients (R = 18, NR = 18) as the derivation cohort were classified into an above group (n = 17) or below group (n = 19) with respect to CLU, VCAM1, and AFP concentrations, depending on whether the rate of change in each protein concentration was above or below the corresponding cutoff value. The above group in the derivation cohort contributed significantly to NR (Supporting Fig. S3C). While 22 patients as the validation cohort were classified into two groups based on the cutoff value for CLU, VCAM1, and AFP concentration, AFP contributed significantly to NR and CLU, showing a tendency to contribute to NR in the validation cohort (Supporting Fig. S3D).

Although VCAM1 and AFP are reportedly involved in the curative effect of SFN, CLU has not been recognized as an early predictor of the response to SFN in patients with HCC.<sup>(17-20)</sup> In addition, data from an interactive open-access database ([www.proteinatlas.org/](http://www.proteinatlas.org/)) and a previous report<sup>(21)</sup> indicate that CLU can be detected in HCC tissues but not in normal liver tissues (Supporting Fig. S4).

A comparison of OS and PFS with the rate of change in CLU concentration in the derivation cohort using a Cox proportional hazards model indicated that an increase in CLU serum level 1 month after treatment initiation was significantly associated with shorter PFS (HR = 2.97,  $P = 0.003$ ) (Supporting Fig. S5A).

## ALTERED SURVIVAL SIGNALING AND METABOLIC STATE IN SORAFENIB-RESISTANT CELLS

We further focused on CLU, an apoptosis-related chaperone protein called apolipoprotein J, because CLU is considered to work as a chemo-resistant in some malignant neoplasms<sup>(22,23)</sup> and be involved in HCC.<sup>(24)</sup> In our examination of the relationship between acquired SFN resistance and CLU expression in cancer cells, we found that HepG2 cells were the most susceptible to SFN among three different cell lines derived from human liver cancer (Fig. 4A). Activation of both cell proliferation (MAPK) and cell

survival (PI3K/Akt) signaling cascades triggered by multiple receptor tyrosine kinases is widely accepted as a major determinant in the development and progression of HCC.<sup>(25,26)</sup> In this context, we confirmed that neither phosphorylation of Erk (p-Erk; activated form of Erk protein) in cell proliferation signaling nor phosphorylation of Akt (p-Akt; activated form of Akt) in cell survival–signaling pathways were substantially activated in HepG2 cells compared with the other cell lines examined (Supporting Fig. S5B). Therefore, we subsequently established HepG2-SR cells by culturing HepG2 cells with long-term exposure to SFN at gradually increasing concentrations. Cell proliferation assays confirmed the SFN-resistant phenotype of these cells, with  $EC_{50}$  values of 1.22  $\mu$ M and 2.13  $\mu$ M in HepG2 and HepG2-SR cells, respectively (Supporting Fig. S5C). In addition, HepG2-SR cells treated with SFN exhibited greater resistance to apoptosis than HepG2 cells (Supporting Fig. S5D).

In HepG2-SR cells, levels of sCLU spliced messenger RNA (mRNA), and sCLU protein in both cell lysate and the supernatant were significantly increased in response to SFN treatment (Fig. 4B–D). Moreover, consistent with these results, immunofluorescence staining indicated that SFN-induced CLU expression was increased in the cytoplasm of HepG2-SR cells, not in the nucleus (Supporting Fig. S5E), suggesting that not nuclear form<sup>(27)</sup> but secretory form of CLU was induced by SFN in the cells. Recent studies have demonstrated that activated PI3K/Akt signaling contributes to acquired SFN resistance,<sup>(28-30)</sup> which is considered to be a compensatory mechanism for blockade of MAPK signaling by SFN. Indeed, Akt protein was activated in response to SFN in both HepG2 and HepG2-SR cells, whereas levels of both p-mTOR protein, a downstream target of the PI3K/Akt signaling pathway, and sCLU protein, increased exclusively in SFN-retreated HepG2-SR cells (Fig. 4C).

To characterize intracellular differences in the response to SFN between HepG2 and HepG2-SR cells, we carried out a gene-expression microarray experiment using both cell lines. We analyzed up-regulated and down-regulated genes in SFN-treated cells exhibiting a >1.5-fold difference in expression compared with vehicle-treated cells using GSEA. Genes associated with metabolism of lipids were significantly enriched in both HepG2 and HepG2-SR cell lines (Fig. 4E and Supporting Fig. S5F–I), whereas

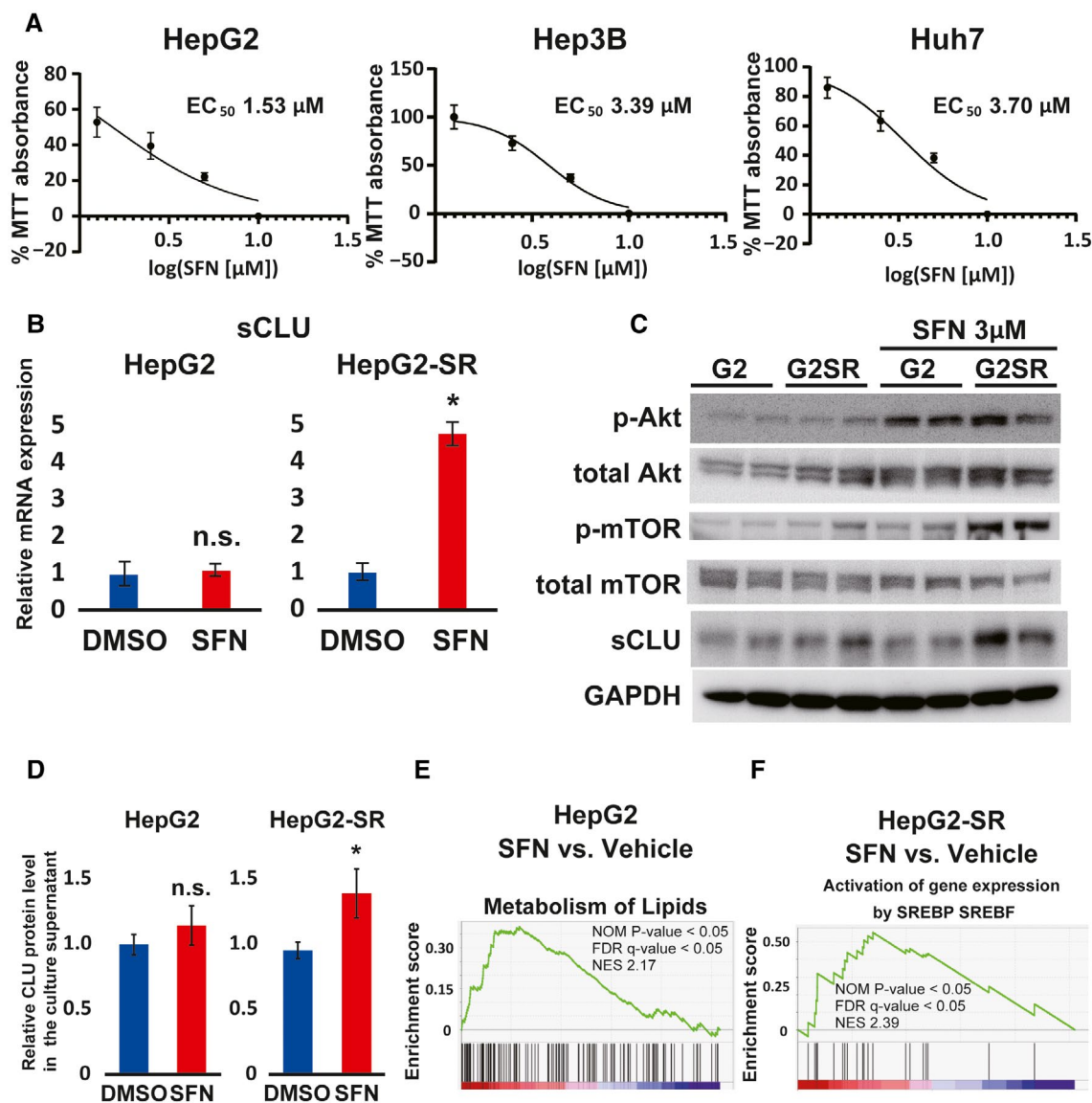


**FIG. 4.** Altered intracellular signaling and metabolic state in HepG2-SR cells. (A) Dose-response curves of HepG2, Huh7, and Hep3B cells treated with increasing doses of SFN at day 5. The  $EC_{50}$  was calculated for each cell line ( $n = 6$ ). (B) Relative sCLU mRNA expression in HepG2 and HepG2-SR cells. Cells were treated with vehicle (DMSO) or 2.5  $\mu$ M SFN for 24 hours ( $n = 3$  in each group). For the SFN treatment experiments using HepG2-SR cells, we challenged HepG2-SR cells with SFN up until 24 hours before the medium change, then cultured with SFN-free regular medium for 24 hours, and subsequently re-treated with vehicle control (DMSO) or SFN for 24 hours (Refer to Materials and Methods). (C) Protein levels of sCLU, phosphorylated Akt (p-Akt), total Akt, phosphorylated mTOR (p-mTOR), total mTOR, and GAPDH detected by western blot analysis in cytoplasmic fraction of HepG2 and HepG2-SR cells. Cells were cultured in regular medium without SFN for 24 hours, and then re-treated with vehicle (DMSO) or 3  $\mu$ M SFN for 24 hours. (D) Relative sCLU protein level in the medium supernatant of HepG2 and HepG2-SR cells. Cells were cultured in regular medium for 24 hours, and then re-treated with vehicle or 2.5  $\mu$ M SFN for 24 hours ( $n = 6$  in each group). (E) Significantly upregulated gene set in HepG2 treated with SFN compared to vehicle control. Changes in the gene expression with a >1.5 fold difference were analyzed between SFN-treated and vehicle (DMSO)-treated HepG2 cells. Full lists of the identified gene sets and each gene are shown in Supporting Fig. S5F and H in the supporting information. (F) Significantly upregulated gene set in SFN-treated HepG2-SR cells compared with vehicle (DMSO) control. Genes exhibiting a >1.5-fold difference in expression level were analyzed between SFN-treated and vehicle-treated HepG2-SR cells. Nominal (NOM) P values and false discovery rates (FDRs) are indicated. Full lists of the identified gene sets and each gene are shown in Supporting Fig. S5G and I in the supporting information. qRT-PCR values were normalized to the expression levels of the *RPLP0* gene. Values are the means  $\pm$  SDs for 3 samples. \* $P < 0.05$  versus DMSO. Abbreviations: NES, Normalized Enrichment Score.

genes associated with activation of gene expression by SREBP SREBF were significantly enriched only in HepG2-SR cells (Fig. 4F, Supporting Fig. S5G,I). These results suggest that the cellular metabolic state adapts to stress induced by SFN, leading to SFN resistance in HepG2-SR cells.

SFN exposure reportedly leads to increases in the cellular adenosine monophosphate-to-adenosine triphosphate (ATP) and adenosine diphosphate (ADP)-to-ATP ratios, signifying an energy deficit,<sup>(31)</sup> and this effect was amplified in HepG2-SR cells (Supporting Fig. S6A). Moreover, SFN treatment increased the cellular ADP-to-ATP ratio in a concentration-dependent manner in HepG2-SR cells (Supporting Fig. S6B). It has been reported that mTOR signaling functions as an excessive energy sensor, and that mTOR and its downstream transcriptional factor, SREBP-1c, are activated under nutrient-rich conditions.<sup>(32)</sup> SFN treatment decreased SREBP-1c expression in HepG2 cells but not in HepG2-SR cells, despite retreatment with SFN (Supporting Fig. S6C). Taking up-regulation of p-mTOR in SFN-retreated HepG2-SR cells (Fig. 4C) into consideration, we have speculated that aberrant mTOR signaling might sustain SREBP-1c expression and account, in part, for up-regulation of CLU in HepG2-SR cells. In addition, using immunofluorescence staining, we observed that SREBP-1 was translocated into the nucleus when HepG2-SR cells were treated with SFN (Supporting Fig. S6D). This finding suggests that SREBP-1c in HepG2-SR cells could be activated by SFN treatment and might partly reflect the result of GSEA analysis that the SREBP-SREBF pathway was enriched in HepG2-SR cells (Supporting Fig. S5I).

Because CLU expression is reportedly regulated by Akt signaling<sup>(33)</sup> and SREBP-1c,<sup>(34,35)</sup> Akt activation, as well as relative activation of mTOR and SREBP-1c induced by SFN administration in HepG2-SR cells, could affect CLU expression. To validate the hypothesized regulatory link between mTOR activation and CLU expression, we treated cells with a PI3K and mTOR inhibitor, BEZ235. HepG2-SR cells were highly susceptible to BEZ235 ( $EC_{50}$  values of 0.23  $\mu$ M and 0.062  $\mu$ M in HepG2 cells and HepG2-SR cells, respectively) (Fig. 5A). In HepG2-SR cells treated with BEZ235, expression levels of SREBP-1c and sCLU mRNA, and sCLU protein, markedly declined (Fig. 5B-D). Furthermore, BEZ235 enhanced the efficacy of SFN in suppressing sCLU expression

(Supporting Fig. S6E,F), cell growth (Supporting Fig. S6G), and sCLU levels in the supernatant (Fig. 5E) in HepG2-SR cells. Moreover, sCLU mRNA expression and protein levels in the supernatant of HepG2-SR cultures increased significantly in control siRNA, whereas SREBP1-knockdown cells treated with SFN did not show a significant difference compared with DMSO (Fig. 5F, Supporting Fig. S6H). We also tried to examine the effect of cell growth by SREBP1 knockdown and confirmed the synergy effect of SREBP1 knockdown for SFN treatment (Supporting Fig. S6I). When we determined the CLU protein level in the culture supernatant, we found that the CLU level was elevated in response to SFN treatment in HepG2-SR and Huh7 cells, which accounts for resistance against SFN treatment (Supporting Fig. S6J). Although Hep3B cells also exhibit a relatively high  $EC_{50}$  for SFN, the CLU level in Hep3B cell supernatants did not increase in response to SFN, indicating that in Hep3B cells p-Akt is constitutively enhanced (Supporting Fig. S5B), accompanied by a high level of CLU protein (Supporting Fig. S6J), leading to resistance against SFN. Functional inhibition of CLU using a specific siRNA prevented cell growth of the hepatoma cell lines and HepG2-SR cells, and enhanced the susceptibility of HCC cell lines to SFN (Supporting Fig. S7A,B), suggesting that sCLU might play an important role not only in the growth of HCC cells but also their acquired resistance to SFN through the compensatory activation of Akt and mTOR/SREBP-1c signaling.

## Discussion

Because our study aimed to establish a blood-based surrogate biomarker without tumor biopsies and an index using parameters from blood examinations for prediction of the therapeutic effect, we focused on the rates of change in the concentration of various serum proteins before and 1 month after the initiation of SFN treatment to reduce the effect of differences in patient backgrounds. The present study indicated that the rate of change in sCLU concentration might be an early predictor of the effect of SFN against HCC. It has been reported that the levels of CLU in plasma fluctuate diurnally in both sexes.<sup>(36)</sup> Because serum was collected at almost the same time in the early morning before meals in the present study, diurnal variation of

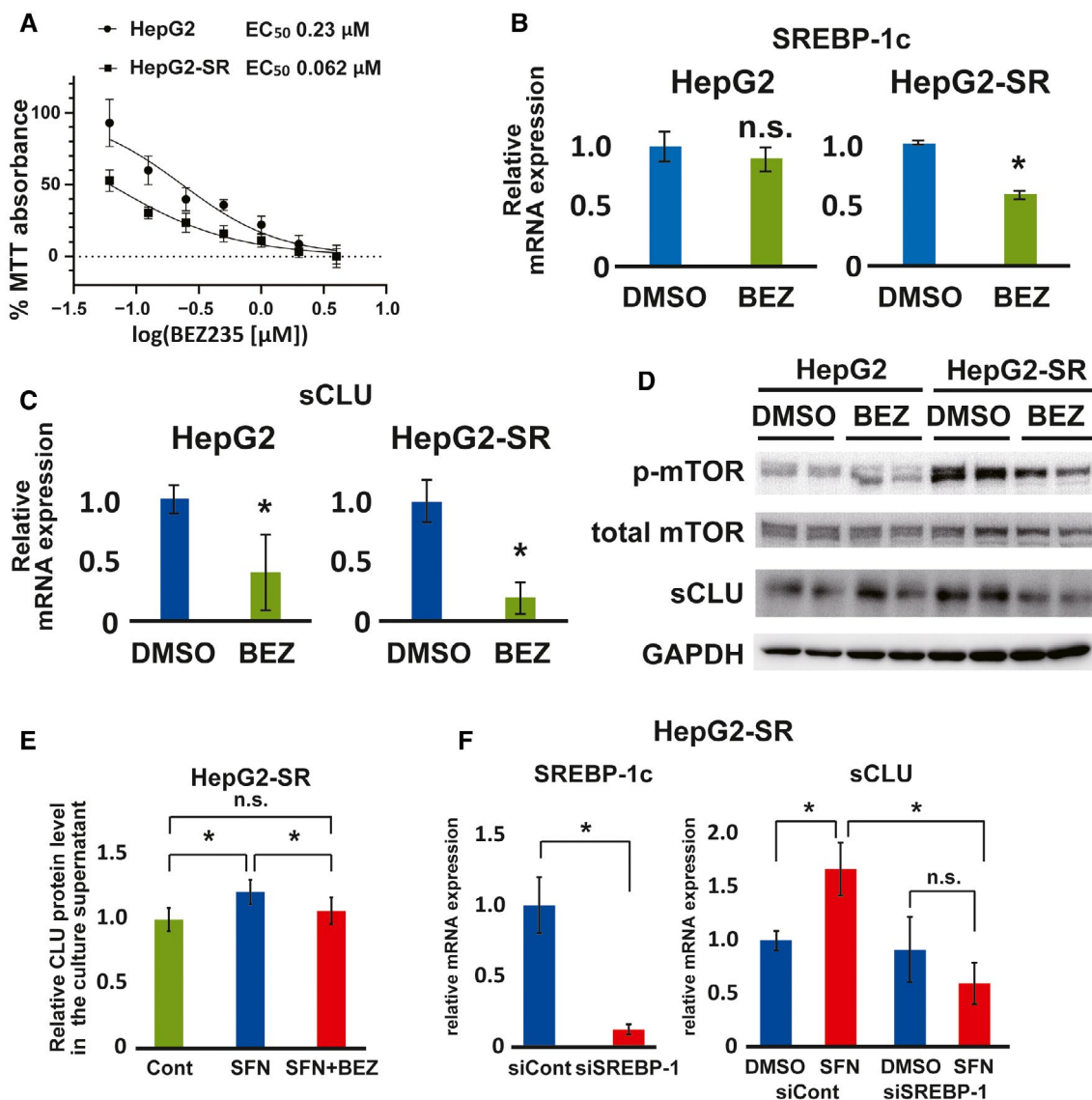


**FIG. 5.** Putative mechanism of SFN resistance in hepatocellular carcinoma. (A) Dose-response curves for HepG2 and HepG2-SR cells treated with increasing doses of the PI3K and mTOR inhibitor BEZ235 (shown as BEZ) at day 5 ( $n = 6$  in each group). (B and C) Relative mRNA expression of SREBP-1c or clusterin in HepG2 and HepG2-SR cells. HepG2-SR cells were treated with SFN up until 24 hours before the medium change. Afterward, cells were treated with vehicle (DMSO) or 0.25  $\mu$ M BEZ235 for 24 hours ( $n = 3$  in each group), followed by quantification of mRNA. (D) Protein levels of phosphorylated mTOR (p-mTOR), total mTOR, sCLU, and GAPDH detected by western blot analysis in cytoplasmic fraction of HepG2 and HepG2-SR cells treated with vehicle (DMSO) or 0.25  $\mu$ M BEZ235 for 24 h. HepG2-SR cells were treated with SFN up until 24 hours before the medium change. (E) Relative sCLU protein level in the culture supernatant of HepG2-SR cells. HepG2-SR cells were treated with SFN up until 1 day before the medium change and then treated with vehicle, 2.0  $\mu$ M SFN, or 2.0  $\mu$ M SFN plus 0.25  $\mu$ M BEZ235 for 24 hours ( $n = 6$  in each group). (F) The efficiency of SREBP-1 knockdown (left panel). SREBP-1 knockdown suppressed CLU expression (right panel). SREBP-depleted HepG2-SR cells were cultured in DMSO or 2.5  $\mu$ M SFN for 24 hours and then quantified mRNA by qRT-PCR. ( $n = 3$  in each group). qRT-PCR values were normalized to the expression level of the *RPLP0* gene. Values are the mean  $\pm$  SD for 2 samples. \* $P < 0.05$  versus control samples (DMSO) unless otherwise stated. For the MTT assay, values are expressed as the mean  $\pm$  SD for 6 samples. Abbreviations: SFN, sorafenib; sCLU, secretory form of clusterin; mTOR, mammalian target of rapamycin.

CLU concentration might not influence the present analysis. According to the *Human Protein Atlas* ([www.proteinatlas.org/ENSG00000120885-CLU/tissue](http://www.proteinatlas.org/ENSG00000120885-CLU/tissue)),

CLU is secreted into the blood by various organs. Among normal organs, the expression of CLU in the liver is relatively low. On the other hand, HCC cells

express CLU protein at different levels (Supporting Fig. S4). We found that CLU was included in the three proteins that were narrowed down among many proteins identified by high-throughput proteome analysis and ELISA, and multivariate analysis including AFP, a specific protein for HCC, also showed a significant difference in CLU. Therefore, serum CLU is considered to be related to HCC.

CLU plays important roles in various pathophysiologic processes including tissue remodeling, reproduction, lipid transport, complement regulation, and apoptosis.<sup>(27,37)</sup> In addition, CLU is reportedly overexpressed in various cancers, such as prostate cancer, pancreatic cancer, melanoma, lung cancer, and breast cancer.<sup>(38-40)</sup> CLU is also thought to be involved in disease progression and metastasis in HCC.<sup>(21,41,42)</sup> Another study of patients with HCC reported a significant association between CLU expression and worse clinical outcome based on parameters such as tumor-node-metastasis stage, histologic malignancy grade, and OS.<sup>(21)</sup> In addition, using two additional serum markers, VCAM1 and AFP, we established an index (NR-index) that enabled prediction of a poor response at 1 month after SFN treatment initiation. As regorafenib and ramucirumab were recently approved as subsequent treatments for patients with SFN-resistant HCC,<sup>(43,44)</sup> the sCLU-related NR-index could greatly contribute to improvement of the prognosis of patients with SFN-resistant HCC by facilitating a switch to the next treatment at an earlier stage. We also examined serum sCLU levels in patients treated with regorafenib and lenvatinib; however, the sCLU levels were not predictive of treatment response (data not shown).

VCAM-1 and AFP were already recognized as prognostic factors for patients with HCC treated with SFN,<sup>(45,46)</sup> but it remains to be elucidated how increased serum CLU levels might be involved in acquired resistance to SFN in HCC. We therefore attempted to clarify the mechanism underlying the relationship between sCLU up-regulation and SFN resistance in HCC. In HCC, both the PI3K/Akt and Raf/Erk signaling pathways are activated; SFN suppresses cancer-cell proliferation primarily by inhibiting the Raf/Erk pathway (Supporting Fig. S8A). We found that sCLU expression increased markedly in HepG2-SR cells in response to SFN treatment (Fig. 4B,C). Both Akt signaling<sup>(33)</sup> and

SREBP-1c<sup>(34,35)</sup> reportedly activate CLU expression. Considering previous literature as well as our findings, we suggest two co-existing mechanisms to explain the up-regulation of sCLU expression in acquired SFN resistance (Supporting Fig. S8A,B). In the first mechanism, inhibition of MAPK signaling by SFN is compensated for by the activation of PI3K/Akt signaling, leading to enhanced CLU expression as shown in Fig 4C, which is supported by previous research.<sup>(28-30)</sup> In the second mechanism, the metabolic dysregulation of SFN-resistant HCC cells, including a relative increase in mTOR activation (Fig. 4C) together with dysregulation of SREBP-1c suppression (Supporting Fig. S6C), is accompanied by subsequent sCLU expression, despite the intracellular energy deficiency, whereas the energy deficiency suppresses mTOR activation and downstream SREBP-1c expression in susceptible HepG2 cells (Fig. 4C, Supporting Fig. S6C). Whichever mechanism predominates, the increase in serum sCLU concentration reflects enhanced CLU expression in HCC tissues of the patients, leading to acquisition of SFN resistance in HCC and a poor clinical outcome.

The PI3K and mTOR inhibitor BEZ235 suppressed sCLU expression and cell growth in HepG2-SR cells (Fig. 5C,D, Supporting Fig. S6G), suggesting that BEZ235 would be useful in treating patients with SFN-resistant, CLU-overexpressing HCC (Supporting Fig. S8C).

These *in vitro* findings indicate that induction of CLU expression may account, at least in part, for SFN resistance and support clinical findings that increased serum CLU concentrations are associated with poor efficacy of SFN treatment in patients with HCC.

Limitations of the present study were that the current findings were based on a single-center retrospective analysis with a small number of cases, leading to low statistical power, which could have affected the accuracy of the results. The findings should be confirmed in a multicenter prospective study.

In conclusion, the sCLU-related NR-index is a promising clinical formula for early prediction of the efficacy of SFN. In addition, sCLU-overexpressing HCC cells may be susceptible to mTOR inhibition; thus, sCLU could be the next promising target in the development of systemic therapies for patients with SFN-resistant HCC.

## REFERENCES

- 1) Bray F, Ferlay J, Soerjomataram I, Siegel RL, Torre LA, Jemal A. Global cancer statistics 2018: GLOBOCAN estimates of incidence and mortality worldwide for 36 cancers in 185 countries. *CA Cancer J Clin* 2018;68:394-424.
- 2) Heimbach JK, Kulik LM, Finn RS, Sirlin CB, Abecassis MM, Roberts LR, et al. AASLD guidelines for the treatment of hepatocellular carcinoma. *Hepatology* 2018;67:358-380.
- 3) Wilhelm S, Carter C, Lynch M, Lowinger T, Dumas J, Smith RA, et al. Discovery and development of sorafenib: a multikinase inhibitor for treating cancer. *Nat Rev Drug Discov* 2006;5:835-844.
- 4) Llovet JM, Ricci S, Mazzaferro V, Hilgard P, Gane E, Blanc J-F, et al. Sorafenib in advanced hepatocellular carcinoma. *N Engl J Med* 2008;359:378-390.
- 5) Cheng A-L, Kang Y-K, Chen Z, Tsao C-J, Qin S, Kim JS, et al. Efficacy and safety of sorafenib in patients in the Asia-Pacific region with advanced hepatocellular carcinoma: a phase III randomised, double-blind, placebo-controlled trial. *Lancet Oncol* 2009;10:25-34.
- 6) Finn RS, Qin S, Ikeda M, Galle PR, Ducreux M, Kim T-Y, et al. Atezolizumab plus bevacizumab in unresectable hepatocellular carcinoma. *N Engl J Med* 2020;382:1894-1905.
- 7) Gordan JD, Kennedy EB, Abou-Alfa GK, Beg MS, Brower ST, Gade TP, et al. Systemic therapy for advanced hepatocellular carcinoma: ASCO guideline. *J Clin Oncol* 2020;38:4317-4345.
- 8) Jackson R, Psarelli EE, Berhane S, Khan H, Johnson P. Impact of viral status on survival in patients receiving sorafenib for advanced hepatocellular cancer: a meta-analysis of randomized phase III trials. *J Clin Oncol* 2017;35:622-628.
- 9) Bruix J, Cheng AL, Meinhardt G, Nakajima K, De Sanctis Y, Llovet J. Prognostic factors and predictors of sorafenib benefit in patients with hepatocellular carcinoma: analysis of two phase III studies. *J Hepatol* 2017;67:999-1008.
- 10) Park J, Cho J, Lim JH, Lee MH, Kim J. Relative efficacy of systemic treatments for patients with advanced hepatocellular carcinoma according to viral status: a systematic review and network meta-analysis. *Target Oncol* 2019;14:395-403.
- 11) Kudo M, Han K-H, Ye S-L, Zhou J, Huang Y-H, Lin S-M, et al. A changing paradigm for the treatment of intermediate-stage hepatocellular carcinoma: Asia-Pacific primary liver cancer expert consensus statements. *Liver Cancer* 2020;9:245-260.
- 12) Shao YY, Hsu CH, Cheng AL. Predictive biomarkers of sorafenib efficacy in advanced hepatocellular carcinoma: are we getting there? *World J Gastroenterol* 2015;21:10336-10347.
- 13) Coate LE, John T, Tsao M-S, Shepherd FA. Molecular predictive and prognostic markers in non-small-cell lung cancer. *Lancet Oncol* 2009;10:1001-1010.
- 14) Nagaoka K, Hino S, Sakamoto A, Anan K, Takase R, Umehara T, et al. Lysine-specific demethylase 2 suppresses lipid influx and metabolism in hepatic cells. *Mol Cell Biol* 2015;35:1068-1080.
- 15) Watanabe T, Ishihara KO, Hirose A, Watanabe S, Hino S, Ojima H, et al. Higher-order chromatin regulation and differential gene expression in the human tumor necrosis factor/lymphotoxin locus in hepatocellular carcinoma cells. *Mol Cell Biol* 2012;32:1529-1541.
- 16) Oniki K, Watanabe T, Kudo M, Izuka T, Ono T, Matsuda K, et al. Modeling of the weight status and risk of nonalcoholic fatty liver disease in elderly individuals: the potential impact of the disulfide bond-forming oxidoreductase A-like protein (DsbA-L) polymorphism on the weight status. *CPT Pharmacometrics Syst Pharmacol* 2018;7:384-393.
- 17) Brown WS, Khalili JS, Rodriguez-Cruz TG, Lizee G, McIntyre BW. B-Raf regulation of integrin alpha4beta1-mediated resistance to shear stress through changes in cell spreading and cytoskeletal association in T cells. *J Biol Chem* 2014;289:23141-23153.
- 18) Personeni N, Bozzarelli S, Pressiani T, Rimassa L, Tronconi MC, Sclafani F, et al. Usefulness of alpha-fetoprotein response in patients treated with sorafenib for advanced hepatocellular carcinoma. *J Hepatol* 2012;57:101-107.
- 19) Yau T, Yao TJ, Chan P, Wong H, Pang R, Fan ST, et al. The significance of early alpha-fetoprotein level changes in predicting clinical and survival benefits in advanced hepatocellular carcinoma patients receiving sorafenib. *Oncologist* 2011;16:1270-1279.
- 20) Nafee AM, Pasha HF, Abd El Aal SM, Mostafa NA. Clinical significance of serum clusterin as a biomarker for evaluating diagnosis and metastasis potential of viral-related hepatocellular carcinoma. *Clin Biochem* 2012;45:1070-1074.
- 21) Zheng W, Yao M, Qian QI, Sai W, Qiu L, Yang J, et al. Oncogenic secretory clusterin in hepatocellular carcinoma: expression at early staging and emerging molecular target. *Oncotarget* 2016;8:52321-52332.
- 22) Koltai T. Clusterin: a key player in cancer chemoresistance and its inhibition. *OncoTargets Therapy* 2014;7:447-456.
- 23) Shannan B, Seifert M, Leskov K, Willis J, Boothman D, Tilgen W, et al. Challenge and promise: roles for clusterin in pathogenesis, progression and therapy of cancer. *Cell Death Differ* 2006;13:12-19.
- 24) Ramadan RA, Madkour MA, El-Nagarr MM, Abourawash SN. Serum clusterin as a marker for diagnosing hepatocellular carcinoma. *Alexandria J Med* 2014;50:227-234. <http://dx.doi.org/10.1016/j.ajme.2014.05.004>.
- 25) Whittaker S, Marais R, Zhu AX. The role of signaling pathways in the development and treatment of hepatocellular carcinoma. *Oncogene* 2010;29:4989-5005.
- 26) Sasaki Y. Insulin resistance and hepatocarcinogenesis. *Clin J Gastroenterol* 2010;3:271-278.
- 27) Lee S, Hong S-W, Min B-H, Shim Y-J, Lee K-U, Lee I-K, et al. Essential role of clusterin in pancreas regeneration. *Dev Dyn* 2011;240:605-615.
- 28) Chen KF, Chen HL, Tai WT, Feng WC, Hsu CH, Chen PJ, et al. Activation of phosphatidylinositol 3-kinase/Akt signaling pathway mediates acquired resistance to sorafenib in hepatocellular carcinoma cells. *J Pharmacol Exp Ther* 2011;337:155-161.
- 29) Zhai BO, Hu F, Jiang X, Xu J, Zhao D, Liu B, et al. Inhibition of Akt reverses the acquired resistance to sorafenib by switching protective autophagy to autophagic cell death in hepatocellular carcinoma. *Mol Cancer Ther* 2014;13:1589-1598.
- 30) Wu CH, Wu X, Zhang HW. Inhibition of acquired-resistance hepatocellular carcinoma cell growth by combining sorafenib with phosphoinositide 3-kinase and rat sarcoma inhibitor. *J Surg Res* 2016;206:371-379.
- 31) Ross FA, Hawley SA, Auciello FR, Gowans GJ, Atrih A, Lamont DJ, et al. Mechanisms of paradoxical activation of AMPK by the kinase inhibitors SU6656 and sorafenib. *Cell Chem Biol* 2017;24:813-824.e814.
- 32) Laplante M, Sabatini DM. mTOR signaling in growth control and disease. *Cell* 2012;149:274-293.
- 33) Zhong B, Sallman DA, Gilvary DL, Pernazza D, Sahakian E, Fritz D, et al. Induction of clusterin by AKT—role in cytoprotection against docetaxel in prostate tumor cells. *Mol Cancer Ther* 2010;9:1831-1841. <http://dx.doi.org/10.1158/1535-7163.mct-09-0880>.
- 34) Kim G, Kim GH, Oh GS, Yoon J, Kim HW, Kim MS, et al. SREBP-1c regulates glucose-stimulated hepatic clusterin expression. *Biochem Biophys Res Commun* 2011;408:720-725.
- 35) Oh GS, Kim G, Yoon J, Kim GH, Kim SW. The E-box-like sterol regulatory element mediates the insulin-stimulated expression of hepatic clusterin. *Biochem Biophys Res Commun* 2015;465:501-506.

- 36) Choi JH, Jeong E, Youn BS, Kim MS. Distinct ultradian rhythms in plasma clusterin concentrations in lean and obese Korean subjects. *Endocrinol Metab (Seoul)* 2018;33:245-251.
- 37) Zhang H, Kim JK, Edwards CA, Xu Z, Taichman R, Wang CY. Clusterin inhibits apoptosis by interacting with activated Bax. *Nat Cell Biol* 2005;7:909-915.
- 38) Shannan B, Seifert M, Leskov K, Boothman D, Pfoehler C, Tilgen W, et al. Clusterin (CLU) and melanoma growth: CLU is expressed in malignant melanoma and 1,25-dihydroxyvitamin D3 modulates expression of CLU in melanoma cell lines in vitro. *Anticancer Res* 2006;26:2707-2716.
- 39) Panico F, Casali C, Rossi G, Rizzi F, Morandi U, Bettuzzi S, et al. Prognostic role of clusterin in resected adenocarcinomas of the lung. *Lung Cancer* 2013;79:294-299.
- 40) Niu ZH, Wang Y, Chun B, Li CX, Wu L. Secretory clusterin (sCLU) overexpression is associated with resistance to preoperative neoadjuvant chemotherapy in primary breast cancer. *Eur Rev Med Pharmacol Sci* 2013;17:1337-1344.
- 41) Kimura A, Sogawa K, Satoh M, Kodera Y, Yokosuka O, Tomonaga T, et al. The application of a three-step serum proteome analysis for the discovery and identification of novel biomarkers of hepatocellular carcinoma. *Int J Proteomics* 2012;2012: 623190.
- 42) Wang C, Jiang K, Kang X, Gao D, Sun C, Li Y, et al. Tumor-derived secretory clusterin induces epithelial-mesenchymal transition and facilitates hepatocellular carcinoma metastasis. *Int J Biochem Cell Biol* 2012;44:2308-2320.
- 43) Bruix J, Qin S, Merle P, Granito A, Huang Y-H, Bodoky G, et al. Regorafenib for patients with hepatocellular carcinoma who progressed on sorafenib treatment (RESORCE): a randomised, double-blind, placebo-controlled, phase 3 trial. *Lancet* 2017;389:56-66.
- 44) Zhu AX, Kang Y-K, Yen C-J, Finn RS, Galle PR, Llovet JM, et al. Ramucirumab after sorafenib in patients with advanced hepatocellular carcinoma and increased  $\alpha$ -fetoprotein concentrations (REACH-2): a randomised, double-blind, placebo-controlled, phase 3 trial. *Lancet Oncol* 2019;20:282-296.
- 45) Kudo M. Biomarkers and personalized sorafenib therapy. *Liver Cancer* 2014;3:399-404.
- 46) Huang D, Yuan W, Li H, Li S, Chen Z, Yang H. Identification of key pathways and biomarkers in sorafenib-resistant hepatocellular carcinoma using bioinformatics analysis. *Exp Ther Med* 2018;16:1850-1858.

Author names in bold designate shared co-first authorship.

## Supporting Information

Additional Supporting Information may be found at [onlinelibrary.wiley.com/doi/10.1002/hep4.1872/supinfo](https://onlinelibrary.wiley.com/doi/10.1002/hep4.1872/supinfo).